Title
Effect of 90° Domain Walls and Thermal Expansion Mismatch on the Pyroelectric Properties of Epitaxial PbZr0.2Ti0.8O3 Thin Films

Journal
Physical Review Letters, 109(25)

ISSN
0031-9007

Authors
Karthik, J
Agar, JC
Damodaran, AR
et al.

Publication Date
2012-12-21

DOI
10.1103/physrevlett.109.257602

Peer reviewed

Effect of 90° Domain Walls and Thermal Expansion Mismatch on the Pyroelectric Properties of Epitaxial $PbZr_{0.2}Ti_{0.8}O_3$ Thin Films

J. Karthik, J. C. Agar, A. R. Damodaran, and L. W. Martin*

Department of Materials Science and Engineering and Materials Research Laboratory, University of Illinois, Urbana-Champaign, Urbana, Illinois 61801, USA

(Received 7 May 2012; published 21 December 2012)

We have investigated the contribution of 90° domain walls and thermal expansion mismatch to pyroelectricity in $PbZr_{0.2}Ti_{0.8}O_3$ thin films. The first phenomenological models to include extrinsic and secondary contributions to pyroelectricity in polydomain films predict significant extrinsic contributions (arising from the temperature-dependent motion of domain walls) and large secondary contributions (arising from thermal expansion mismatch between the film and the substrate). Phase-sensitive pyroelectric current measurements are applied to model thin films for the first time and reveal a dramatic increase in the pyroelectric coefficient with increasing fraction of in-plane oriented domains and thermal expansion mismatch.

DOI: 10.1103/PhysRevLett.109.257602 PACS numbers: 77.55.Kt, 64.60.Ej, 77.70.+a, 77.80.bn

Pyroelectricity, the temperature dependence of spontaneous polarization in ferroelectrics, enables a variety of devices [1–3] which utilize the pyroelectric current or voltage developed in response to temperature fluctuations. Traditionally, these systems relied on bulk materials, but future nanoscale devices will increasingly require ferroelectric thin films. Reducing the dimensions of ferroelectrics increases their susceptibility to size- and strain-induced effects. In this spirit, thin-film epitaxy has been developed to provide a set of parameters (e.g., film composition, epitaxial strain, electrical boundary conditions, and thickness [4,5]) that allow for precise control of ferroelectrics and has been instrumental in understanding dielectric and piezoelectric effects. However, measuring the pyroelectric response of thin films is difficult and has restricted the understanding of the physics of pyroelectricity, prompting some to label it as ''one of the least-known properties of solid materials'' [6].

In general, the pyroelectric properties of a ferroelectric under short-circuit conditions are affected by three contributions: intrinsic, extrinsic, and secondary. The *intrinsic* contribution arises from a temperature-dependent change in the polarization in the bulk of a ferroelectric domain. The *extrinsic* contribution arises from the temperature-dependent movement of domain walls in a polydomain state. The sum of these two coefficients is referred to as the *primary* pyroelectric coefficient. Since pyroelectric materials are also piezoelectric, thermal expansion results in pyroelectricity which is referred to as a *secondary* contribution. In thin-film samples, this secondary contribution is related to the difference in thermal expansion between the film and substrate [7]. In general, one might expect the extrinsic effect to be qualitatively analogous to the domain wall contributions observed in dielectric and piezoelectric properties;[8,9] however, recent theoretical work [10] suggests that extrinsic contributions to pyroelectricity are actually qualitatively different and can be large in magnitude (comparable to intrinsic contributions). Such observations remain experimentally unstudied. On the other hand, the effect of thermal expansion mismatch is generally ignored for dielectrics and piezoelectrics as the sample is assumed to remain at a constant temperature and little experimental work has been completed on this contribution to pyroelectricity.

As noted, experimental limitations have restricted widespread study of pyroelectricity in thin films. Most measurement techniques were developed to probe bulk ceramics or single crystals, including laser induced heating [11] and constant ramp-rate heating induced current measurements [12]. These techniques are adequate to identify pyroelectricity or to estimate the pyroelectric coefficients of large samples, but lack precision as a consequence of poor temperature accuracy, nonuniform heating, and contributions from thermally stimulated currents [13]. Regardless, these techniques have been applied, with limited success, to characterize thin films [14–17]. Phase-sensitive techniques [18,19] overcome some of these limitations and provide an accurate measure of pyroelectricity. This method is, however, difficult to implement on small-area (< 200 μm diameter) thin-film ferroelectric capacitors whose pyroelectric current can be small (~ 100 fA for $dT/dt = 1 - 10$ K/min.). To our knowledge, pyroelectric measurements using a phase-sensitive technique have not been reported on such thin-film capacitors. It is these measurement limitations that have, in turn, limited a deeper understanding of pyroelectricity.

Using a combination of thin-film epitaxy, phase-sensitive, low-noise variable temperature electrical measurements, and Ginzburg-Landau-Devonshire (GLD) models, we investigate the intrinsic, extrinsic, and secondary contributions to pyroelectricity in polydomain $PbZr_{0.2}Ti_{0.8}O_3$ films. Extrinsic and secondary contributions

are found to greatly impact pyroelectricity near room temperature—with the pyroelectric coefficient increasing by 25%–50% with increasing fraction of in-plane oriented domains and thermal expansion mismatch. In the remainder of this Letter we develop a framework to understand the various contributions to pyroelectricity.

Ferroelectric materials form complex domain structures to minimize electrostatic and elastic energies [20,21]. In films of tetragonal ferroelectrics such as $PbZr_{0.2}Ti_{0.8}O_3$, these interactions result in the formation of c and a domains (with their tetragonal axes along or perpendicular to the substrate normal, respectively) that are separated by 90° domain walls ($c/a/c/a$ structure). The volume fraction of the c and a domains at any temperature can be controlled by modifying the elastic boundary conditions via epitaxial strain [22–24]. Large compressive strains reinforce tetragonality and form monodomain, c-axis oriented structures. Decreasing compressive strain (or increasing thickness) results in a strain driven relaxation to the $c/a/c/a$ structure where the fraction of the in-plane oriented a domains increases until, at a critical tensile strain, the entire film transforms to an in-plane oriented $a_1/a_2/a_1/a_2$ structure.

Here the thermodynamic properties of these films are calculated using a polydomain GLD model that for the first time includes both extrinsic contributions arising from temperature-dependent domain wall movement and secondary contributions arising from thermal expansion mismatch with the substrate [10,22,23]. It has been shown that in the case of thick ferroelectric films with dense domain structures (such as those studied herein) that the polarization and stress fields can be assumed to be homogeneous within each domain thereby greatly simplifying the complexity of the models [22,25,26]. A complete discussion of the GLD functional, the boundary conditions, and the equations of state are provided in the Supplemental Material [27]. The pyroelectric coefficient along the [001] can be defined as $\pi_3 = \frac{d\langle P_3\rangle}{dT}$, where $\langle P_3\rangle = \phi_c P_s$, ϕ_c is the volume fraction of the c domains, and P_s is the spontaneous polarization. The total pyroelectric coefficient can be expressed as $\pi_3 = \phi_c \frac{dP_s}{dT} + P_s \frac{d\phi_c}{dT}$ [10], where the first and second terms represent the *intrinsic* and *extrinsic* contribution to the pyroelectric coefficient, respectively. Using such a model, the pyroelectric coefficient of a $PbZr_{0.2}Ti_{0.8}O_3$ thin film at 320 K was calculated [Fig. 1]. The intrinsic response [orange line, Fig. 1] is found to be negative for all domain configurations with $P_3 \neq 0$ and is maximized at the boundary between the c and $c/a/c/a$ structures. Additionally, the extrinsic contribution due to the temperature-induced motion of 90° domain walls was calculated [green line, Fig. 1]. Note that the extrinsic contribution occurs exclusively in the $c/a/c/a$ structure and the sign of the extrinsic contribution depends on the nature of the epitaxial strain (with compressive and tensile strains resulting in positive and negative contributions,

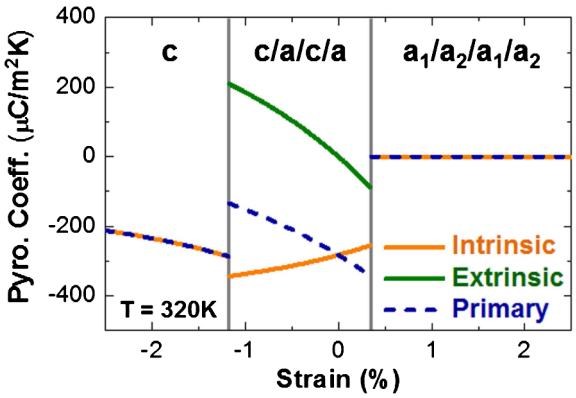

FIG. 1 (color online). Equilibrium domain structure and pyroelectric coefficients of $PbZr_{0.2}Ti_{0.8}O_3$ thin films calculated using polydomain GLD theory at 320 K. The solid orange line shows the intrinsic pyroelectric coefficient, the solid green line (at the top in the c/a/c/a section) shows the extrinsic contribution to the pyroelectric coefficient from the 90° domain walls, and the dashed blue line shows the primary (intrinsic and extrinsic) pyroelectric coefficient.

respectively). Thus, the primary pyroelectric coefficient is maximized at a tensile strain corresponding to the transition that accompanies the disappearance of the c domains [dashed line, Fig. 1]. The presence of domain walls results in a shift of the position of maximum pyroelectric coefficient from compressive to tensile strain and the pyroelectric coefficient is observed to increase with increasing density of the a domains until the film is completely in-plane polarized. This strain-dependent sign of the extrinsic contribution is very different from the analogous effects in dielectric and piezoelectric responses. In those cases, the 90° domain walls are predicted and observed to enhance the susceptibility of the material to applied electric field or stress (regardless of strain state). In the case of pyroelectricity, however, the sign of the applied epitaxial strain has significant impact on the nature of the domain wall motion to changing temperature. This fact had not been previously appreciated from more simplistic models.

To experimentally probe the pyroelectricity, we have grown 150 nm $PbZr_{0.2}Ti_{0.8}O_3$/20 nm $SrRuO_3$ heterostructures on $SrTiO_3$(001), $DyScO_3$(110), $TbScO_3$(110), and $GdScO_3$(110) substrates (which provide a lattice mismatch of −0.8%, 0.2%, 0.6%, and 0.9%, respectively, with $PbZr_{0.2}Ti_{0.8}O_3$) using pulsed-laser deposition [28]. $SrRuO_3$ was used as a lattice-matched bottom electrode on all substrates and symmetric capacitor structures were fabricated by depositing an 80 nm thick epitaxial $SrRuO_3$ top electrode (circular capacitors, diameter 25–100 μm) patterned using an MgO-based hard-mask process [29]. Atomic force microscopy of as-grown films revealed smooth surfaces with root-mean-square roughness <1 nm and x-ray diffraction studies revealed single-phase, fully epitaxial thin films [Fig. 2(a)]. An increase in ϕ_a from ~4% for films grown on $SrTiO_3$ to ~20% for films grown on

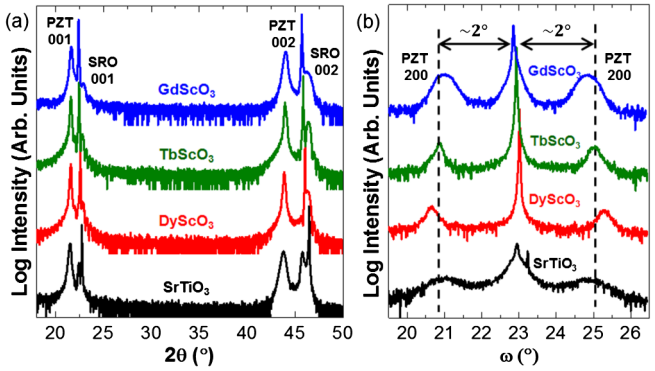

FIG. 2 (color online). (a) θ-2θ x-ray diffraction patterns for various thin film heterostructures reveal single-phase, epitaxial films on all substrates. (b) Specular ω-rocking curves about the 200 diffraction peak of $PbZr_{0.2}Ti_{0.8}O_3$ reveal an increasing fraction of a domains with increasing tensile strain from $SrTiO_3$ to $GdScO_3$.

$GdScO_3$, consistent with the GLD models, was observed using x-ray diffraction rocking curve studies [30] [Fig. 2(b)] and piezoresponse force microscopy (Supplemental Material, Fig. S1 [27]). These films provide a model system, spanning the $c/a/c/a$ polydomain region of the $PbZr_{0.2}Ti_{0.8}O_3$ system, with which to probe the various contributions to pyroelectricity.

The pyroelectric current (i_p) from a ferroelectric capacitor depends on the rate of change of temperature as $i_p = \pi A \frac{dT}{dt}$, where π is the pyroelectric coefficient and A is the area of the capacitor. In contrast, within a narrow temperature interval (a few degrees K), the thermally stimulated current (i_s) depends on the temperature linearly as $i_s = i_{so} + \lambda T$ where i_{so} is the room temperature thermally stimulated current and λ is a constant related to the activation energy of the trap states that give rise to the thermally stimulated currents [18]. Therefore, in response to a sinusoidal temperature oscillation, the component of the current in-phase with the temperature is related to the thermally stimulated current [18,19] and the current out of phase with the temperature is the pyroelectric current.

Phase-sensitive measurements of the pyroelectric coefficient were completed by measuring the current induced in response to sinusoidal temperature oscillations using a current preamplifier (Femto DLPCA-200) mounted in close proximity to the sample [Fig. 3(a)]. Temperature variations of the form $T = T_b + T_0 \sin(\omega t)$ with a background temperature $T_b = 320$ K and oscillations of magnitude $T_0 \sim 1.25$ K at an angular frequency $\omega \approx 0.125$ rad/s were utilized to obtain a clean sinusoidal oscillation in a stable temperature near room temperature while producing a pyroelectric current that can be measured accurately [Figs. 3(b) and 3(c)]. The pyroelectric coefficient was extracted from the out-of-phase component of the measured sinusoidal current as [19] $\pi = \frac{i_0 \sin(\theta)}{A T_0 \omega}$ where i_0 is the amplitude of the current oscillation and θ

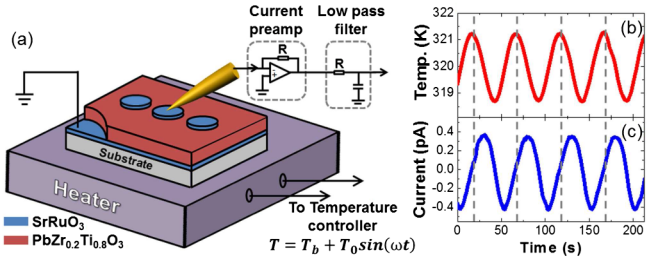

FIG. 3 (color online). (a) Schematic of the phase-sensitive measurement technique utilizing a sinusoidal temperature oscillation. (b) Typical trace of the applied temperature variation and (c) the measured sinusoidal pyroelectric current on a 100 μm diameter $PbZr_{0.2}Ti_{0.8}O_3$ capacitor.

is the measured phase difference between the current and the temperature oscillations. The pyroelectric coefficient was extracted from a large number ($n = 32$) of capacitors from a minimum of two identically prepared samples on each substrate. The measured phase difference θ between the temperature and current oscillations is close to $-90°$ in all samples as expected; see the Supplemental Material, Fig. S2 [27]. Deviations from $-90°$ phase difference between the temperature and current oscillations likely arise due to the presence of thermally stimulated currents in these samples; however, our ability to precisely measure the phase difference allows us to unequivocally identify the purely pyroelectric contribution.

These studies reveal that, as ϕ_a increases from ~4% to ~20%, the measured pyroelectric coefficient increases from ~ -200 to -300 $\mu C/m^2$ K [Fig. 4]. This is consistent with the predictions that the primary pyroelectric

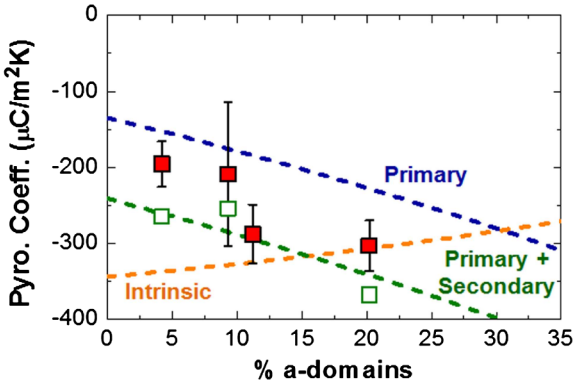

FIG. 4 (color online). The measured pyroelectric coefficient (filled red squares) as a function of percentage a-domains in polydomain $PbZr_{0.2}Ti_{0.8}O_3$ thin films. The dashed orange line is the intrinsic response and the dashed blue line is the primary response (intrinsic + extrinsic) calculated using polydomain GLD theory. The open green squares indicate the sum of primary + secondary contributions to the pyroelectric coefficient for each film-substrate combination and the dashed green line indicates the trend expected assuming an average thermal expansion coefficient of 10.9×10^{-6} K^{-1} for all the substrates.

response should increase with the density of 90° domain walls (since there are more domain walls to provide extrinsic contributions). This indicates that the monodomain models of intrinsic response are inadequate to explain the observed pyroelectric response in polydomain films. The measured pyroelectric coefficient, however, shows a minor, but systematic, deviation from the values predicted for the primary contribution (i.e., measured values are consistently larger). While it is unrealistic to expect the GLD theory to provide a precise prediction of the actual pyroelectric coefficients, it is possible that the systematic deviation arises from other mechanisms active in thin-film ferroelectrics. As discussed previously, thin films are susceptible to secondary effects due to thermal expansion mismatch between the film and substrate. In prior work, such secondary contributions have been estimated to play a minor role in the pyroelectric response of thin films ($< 10\%$ of the total response, except near the morphotropic phase boundary) [7]. However, such models have only investigated monodomain ferroelectric thin films. Here, we calculate the secondary contribution to the pyroelectric coefficient in polydomain films and show that it can significantly enhance pyroelectricity. Since the polarization also depends on the strain due to the thermal expansion mismatch, we can write the secondary contribution as $\pi_s = \frac{\partial \langle P_3 \rangle}{\partial u_m} \frac{\partial u_m}{\partial T}$, where u_m is the misfit strain with the substrate. Using the temperature dependence of the lattice constants π_s can be simplified as [27]

$$\pi_s = (u_m - 1)(\alpha_f - \alpha_s)\left\{\phi_c \frac{\partial P_s}{\partial u_m} + P_s \frac{\partial \phi_c}{\partial u_m}\right\}, \quad (1)$$

where α_f and α_s are the thermal expansion coefficients of the film and the substrate, respectively. This can be used to calculate the secondary contribution to the pyroelectric coefficient of polydomain thin films from the strain dependence of P_s and ϕ_c [22]. The average in-plane thermal expansion coefficients of $SrTiO_3$, $DyScO_3$, and $GdScO_3$ are 11.1×10^{-6}, 9.3×10^{-6}, and 12.1×10^{-6} K^{-1}, respectively [31,32]. Experimental measurement of the thermal expansion coefficient of $TbScO_3$ is not available in the literature. We can observe general trends by using an average thermal expansion coefficient for all substrates studied here (10.9×10^{-6} K^{-1}) and PZT (5.4×10^{-6} K^{-1}) [31]. Using these values, we estimated the average secondary contribution to the pyroelectric coefficient [dashed green line, Fig. 4]. We see that the effect of the thermal expansion mismatch is more significant in the polydomain state as compared to a monodomain state due to the sensitive strain dependence of ϕ_c. The secondary contribution contributes an additional 25%–50% to the total room-temperature response and provides an important correction to the primary pyroelectric coefficient calculated previously. Alternatively, we can consider each film-substrate combination independently (done here for films on $SrTiO_3$, $DyScO_3$, and $GdScO_3$ substrates) [open green squares, Fig. 4]. This approach helps explain the fine-structure observed in the data (relative vertical shifts of data points) and reveals that the secondary contribution is a complex and potentially large additional contribution.

Nevertheless, the addition of the secondary effect seems to systematically exceed the values of the measured pyroelectric coefficients. This could arise for a number of possible reasons. (i) Domain wall effects are overestimated due to domain wall pinning resulting in a lower extrinsic contribution than expected from GLD theory. The diminished extrinsic contributions push responses closer to the intrinsic values, thereby increasing the magnitude of the response in the region of interest. (ii) The secondary effects require further corrections (due to, for example, anisotropic thermal expansion coefficients). Nonetheless, this work has provided the first comprehensive study of pyroelectricity in polydomain ferroelectric thin films with $c/a/c/a$ domain structures. This insight dramatically improves the current understanding of extrinsic (domain wall) and secondary contributions to pyroelectricity and how thin-film epitaxy can be used to generate model systems for the study of this underdeveloped realm of materials physics. Such thin-film approaches could also be utilized to explore additional exciting observations concerning pyroelectricity in nonpolar ferroelastics and nanoscale ferroelectrics which have been recently reported [33–35].

In conclusion, this work has investigated the various contributions to pyroelectricity in ferroelectric thin films. We have demonstrated the crucial role played by 90° domain walls and thermal expansion mismatch on pyroelectricity. In general, a dramatic increase in the pyroelectric coefficient with increasing fraction of in-plane oriented domains and thermal expansion mismatch is observed. The extrinsic contribution to pyroelectricity from domain walls is found to be distinctly different from the analogous effects in dielectric and piezoelectric responses in that the sign of the effect depends on the nature of the applied epitaxial strain. At the same time, due to the strong coupling between the polarization and the lattice, the thermal expansion mismatch between film and substrate is also found to be strongly active in polydomain films providing an additional 25%–50% enhancement of pyroelectricity. These observations have important implications for the temperature dependent response of ferroelectrics and have not been previously probed either in models or experiment.

J. K. and L. W. M. acknowledge support from the Office of Naval Research under Grant No. N00014-10-10525. A. R. D. and L. W. M. acknowledge support from the Army Research Office under Grant No. W911NF-10-1-0482. J. A. and L. W. M. acknowledge support from the Air Force Office of Scientific Research under Grant No. AF FA 9550-11-1-0073. Experiments were carried out in part in the Frederick Seitz Materials Research Laboratory Central Facilities, University of Illinois, Urbana-Champaign.

*lwmartin@illinois.edu

[1] M. E. Lines and A. M. Glass, *Principles and Applications of Ferroelectrics and Related Materials* (Oxford University Press, New York, 1979).

[2] R. W. Whatmore, Rep. Prog. Phys. **49**, 1335 (1986).

[3] R. B. Olsen, D. A. Bruno, and J. M. Briscoe, J. Appl. Phys. **58**, 4709 (1985).

[4] M. Dawber, K. M. Rabe, and J. F. Scott, Rev. Mod. Phys. **77**, 1083 (2005).

[5] D. G. Schlom, L.-Q. Chen, C.-B. Eom, K. M. Rabe, S. K. Streiffer, and J.-M. Triscone, Annu. Rev. Mater. Res. **37**, 589 (2007).

[6] S. B. Lang, Phys. Today **58**, 31 (2005).

[7] J. D. Zook and S. T. Liu, J. Appl. Phys. **49**, 4604 (1978).

[8] F. Xu, S. Trolier-McKinstry, W. Ren, B. Xu, Z.-L. Xie, and K. J. Hemker, J. Appl. Phys. **89**, 1336 (2001).

[9] Q. M. Zhang, H. Wang, N. Kim, and L. E. Cross, J. Appl. Phys. **75**, 454 (1994).

[10] J. Karthik and L. W. Martin, Phys. Rev. B **84**, 024102 (2011).

[11] A. G. Chynoweth, J. Appl. Phys. **27**, 78 (1956).

[12] R. L. Byer and C. B. Roundy, Ferroelectrics **3**, 333 (1972).

[13] S. Zhao, S. J. Zhang, W. Liu, N. J. Donnelly, Z. Xu, and C. A. Randall, J. Appl. Phys. **105**, 053705 (2009).

[14] R. Bruchhaus, D. Pitzer, M. Schreiter, and W. Wersing, J. Electroceram. **3**, 151 (1999).

[15] R. Takayama and Y. Tomita, J. Appl. Phys. **65**, 1666 (1989).

[16] Q. Zhang and R. W. Whatmore, J. Phys. D **34**, 2296 (2001).

[17] W. Liu, J. S. Ko, and W. Zhu, Thin Solid Films **371**, 254 (2000).

[18] L. E. Garn and E. J. Sharp, J. Appl. Phys. **53**, 8974 (1982).

[19] L. E. Garn and E. J. Sharp, J. Appl. Phys. **53**, 8974 (1982).

[20] B. S. Kwak, A. Erbil, B. J. Wilkens, J. D. Budai, M. F. Chrisholm, and L. A. Boatner, Phys. Rev. Lett. **68**, 3733 (1992).

[21] C. M. Foster, W. Pompe, A. C. Daykin, and J. S. Speck, J. Appl. Phys. **79**, 1405 (1996).

[22] V. G. Koukhar, N. A. Pertsev, and R. Waser, Phys. Rev. B **64**, 214103 (2001).

[23] V. G. Kukhar, N. A. Pertsev, H. Kohlstedt, and R. Waser, Phys. Rev. B **73**, 214103 (2006).

[24] J. Karthik, A. R. Damodaran, and L. W. Martin, Phys. Rev. Lett. **108**, 167601 (2012).

[25] C. S. Ganpule, V. Nagarajan, B. K. Hill, A. L. Roytburd, E. D. Williams, R. Ramesh, S. P. Alpay, A. Roelofs, R. Waser, and L. M. Eng, J. Appl. Phys. **91**, 1477 (2002).

[26] N. A. Pertsev and A. G. Zembilgotov, J. Appl. Phys. **78**, 6170 (1995).

[27] See Supplemental Material at http://link.aps.org/supplemental/10.1103/PhysRevLett.109.257602 for a detailed description of the Ginzburg-Landuan-Devonshire models used in this work, piezoresponse force microscopy images of the various samples, and additional details of the phase-sensitive pyroelectric measurements.

[28] The $SrRuO_3$ and $PbZr_{0.2}Ti_{0.8}O_3$ layers were fabricated by pulsed laser deposition employing a KrF excimer laser (wavelength $\lambda = 248$ nm) from ceramic $SrRuO_3$ and $Pb_{1.1}Zr_{0.2}Ti_{0.8}O_3$ targets (Praxair Specialty Ceramics). The $SrRuO_3$ layer (20 nm) was deposited at 630 °C in an oxygen pressure of 100 mTorr, with a laser fluence of 1.75 J/cm^2 at a laser repetition rate of 12 Hz. The subsequent $PbZr_{0.2}Ti_{0.8}O_3$ layer (150 nm) was grown at 630 °C in an oxygen pressure of 200 mTorr at a laser fluence of 2 J/cm^2 and a laser repetition rate of 3 Hz.

[29] J. Karthik, A. R. Damodaran, and L. W. Martin, Adv. Mater. **24**, 1610 (2012).

[30] V. Nagarajan, I. G. Jenkins, S. P. Alpay, H. Li, S. Aggarwal, L. Salamanca-Riba, A. L. Roytburd, and R. Ramesh, J. Appl. Phys. **86**, 595 (1999).

[31] H. Nakaki, Y. K. Kim, S. Yokoyama, R. Ikariyama, H. Funakubo, K. Nishida, K. Saito, H. Morioka, O. Sakata, H. Han, and S. Baik, J. Appl. Phys. **105**, 014107 (2009).

[32] M. D. Biegalski, J. H. Haeni, S Troiler-McKinstry, D. G. Schlom, C. D. Brandle, and A. J. V. Graitis, J. Mater. Res. **20**, 952 (2005).

[33] A. N. Morozovska, E. A. Eliseev, M. D. Glinchuk, L.-Q. Chen, and V. Gopalan, Phys. Rev. B **85**, 094107 (2012).

[34] A. N. Morozovska, E. A. Eliseev, S. V. Kalinin, L.-Q. Chen, and V. Gopalan, Appl. Phys. Lett. **100**, 142 902 (2012).

[35] A. N. Morozovska, E. A. Eliseev, G. S. Svechnikov, and S. V. Kalinin, J. Appl. Phys. **108**, 042009 (2010).